Available online at www.sciencedirect.com

ScienceDirect

Mendeleev Commun., 2021, **31**, 475–477

Mendeleev Communications

Phosphite-containing iridium polarization transfer catalysts for NMR signal amplification by reversible exchange

Kirill A. Spiridonov,[a,b] Vitaly P. Kozinenko,[c,d] Igor A. Nikovsky,[a] Alexander A. Pavlov,[a,e] Tatyana N. Vol'khina,[a] Yulia V. Nelyubina,[a,f] Alexey S. Kiryutin,[c,d] Alexandra V. Yurkovskaya,[c,d] Alexander A. Polezhaev,[a,f] Valentin V. Novikov*[a,e] and Konstantin L. Ivanov†[,c,d]

[a] *A. N. Nesmeyanov Institute of Organoelement Compounds, Russian Academy of Sciences, 119991 Moscow, Russian Federation. E-mail: novikov84@ineos.ac.ru*
[b] *Department of Chemistry, M. V. Lomonosov Moscow State University, 119991 Moscow, Russian Federation*
[c] *International Tomography Center, Siberian Branch of the Russian Academy of Sciences, 630090 Novosibirsk, Russian Federation*
[d] *Novosibirsk State University, 630090 Novosibirsk, Russian Federation*
[e] *Moscow Institute of Physics and Technology, 141701 Dolgoprudny, Moscow Region, Russian Federation*
[f] *Bauman Moscow State Technical University, 105005 Moscow, Russian Federation*

DOI: 10.1016/j.mencom.2021.07.012

Two new iridium complexes with an N-heterocyclic carbene and phosphite ligands have been synthesized and characterized. Bubbling of parahydrogen through their solutions resulted in the formation of several hydride complexes. In the presence of pyridine, this process is accompanied by transfer of spin order from the molecular hydrogen to pyridine molecules undergoing dynamic exchange between free and complex-bound states.

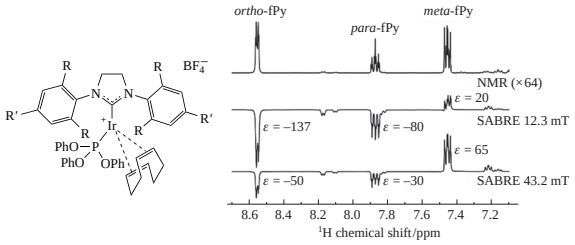

Keywords: iridium complexes, carbene ligands, parahydrogen, hyperpolarization, NMR spectroscopy.

Nuclear magnetic resonance (NMR) spectroscopy is one of the most powerful tools for a wide range of applications, from chemistry and physics to structural biology and medical diagnostics. The main obstacle for an even more wide-spread use of NMR spectroscopy is its low sensitivity, which results from an extremely small difference in populations of nuclear spin states at room temperature, typically being of the order of 10^{-5}–10^{-4}. Overcoming this fundamental limitation could lead to a revolution[1–3] in magnetic resonance spectroscopy and imaging, as it would provide the tool for a quantitative visualization of metabolic processes occurring inside a living organism and thus, for early diagnosis of related pathologies.[4–6] To improve the sensitivity of NMR spectroscopy, several approaches can be used for increasing the above difference in populations (ideally, to unity), *i.e.*, for achieving a so-called hyperpolarization. One of such approaches makes use of spin order of the parahydrogen molecule, which is an H_2 molecule in a singlet nuclear spin state, as a source of hyperpolarization and of suitable chemical reactions to generate strongly enhanced signals in the NMR spectra, the so-called parahydrogen-induced nuclear polarization (PHIP).[7–10] A classical variant of this effect exploits hydrogenation of unsaturated substrates with parahydrogen in the presence of homogeneous[11,12] or, in some cases, heterogeneous[13] catalysts.

A decade ago,[14] a new approach, Signal Amplification by Reversible Exchange (SABRE), has emerged, which is based on reversible interaction of the parahydrogen molecule with an iridium center of a homogeneous catalyst, resulting in the transfer of polarization from the coordinated parahydrogen molecule to nuclei of other ligands[15,16] that are typically small heterocyclic species, *e.g.*, pyridine. These labile ligands can act as nucleophiles and undergo an exchange between their free and complex-bound forms in a solution. Since the time of the first publications,[14,17] many iridium complexes (mostly carbene-based) were recognized as suitable for use in the SABRE technique.[18–25] Among other reasons, there is an efficiency of polarization transfer that is affected by such factors as lifetimes of hydride intermediate complexes and a number of analyte molecules allowed to enter the coordination sphere of the iridium ion,[26,27] both amenable to molecular design by a proper choice of organic ligands. As an example, a phosphine moiety incorporated into a SABRE catalyst was used by Duckett to tune the polarization transfer and to identify key intermediates of the process.[28]

In this work, we make a further step towards expanding the 'toolkit' of SABRE catalysts by obtaining two new iridium complexes, $[Ir(COD)P(OPh)_3(SIMes)][BF_4]$ **1** and $[Ir(COD)P(OPh)_3(SIPr)][BF_4]$ **2**, with different N-heterocyclic carbenes and phosphite ligands (Scheme 1).[29–32] They were synthesized by substituting the coordinated chloride ion in the corresponding precursor complexes by subsequently treating them with silver tetrafluoroborate and triphenyl phosphite (Scheme 1, also see Supplementary Materials for more details).

The formation of the target complexes **1** and **2** has been confirmed (with some issues in the latter case, as explained below) by X-ray diffraction analysis of their single

† Deceased.

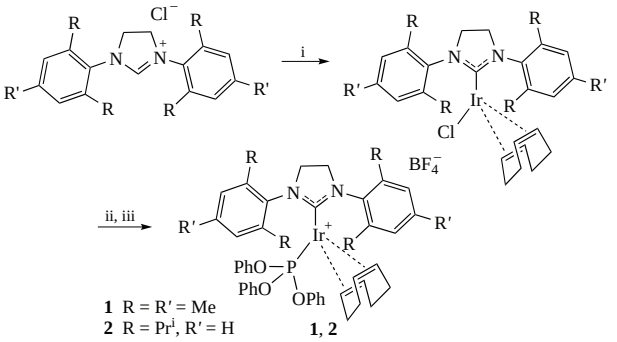

Scheme 1 *Reagents and conditions*: i, $[Ir(COD)Cl]_2$, Bu^{t}OK, THF; ii, $AgBF_4$, acetone; iii, $P(OPh)_3$, THF.

crystals‡ obtained by a diffusion of Et_2O vapor into THF solutions on air. As follows from the unambiguous results for **1** (Figure 1), an overall molecular geometry of this complex is rather expected for such type of iridium compounds. Among others, the bond lengths Ir(1)–P(1) and P(1)–O are close to the mean values of 2.250 and 1.591 Å in iridium complexes with an $IrP(OX)_3$ moiety in Cambridge Structural Database, version 5.41 (November 2019). In contrast, the Ir–C bonds to SIMes and COD ligands are longer by 0.04 Å in average than their mean values in the respective complexes separately featuring $C_3N_2H_4$ (2.040 Å) and COD (2.163 Å) fragments, which may be attributed to the steric bulk of these two ligands simultaneously bound to the same metal ion in **1**.

For complex **2**, however, the X-ray diffraction data identified a coexistence of three different complexes in a 3:1:4 ratio, $[Ir(COD)P(OPh)_3(SIPr)][BF_4]$ and its two by-products, $[Ir(COD)P(OPh)_2(OH)(SIPr)][BF_4]$ and $[Ir(COD)P(OPh)_2(O)(SIPr)]$ with an OH group and an O^- moiety instead of one phenyl group in the triphenyl phosphite ligand (see Online Supplementary Materials, Figure S1). The latter two complexes, apparently, resulted from the hydrolysis of the target product **2** upon its prolonged crystallization in air, as the NMR spectra collected from its solution before the attempted crystallization did not suggest the presence of such admixtures. For more details on the crystal structure, see Figure S1.

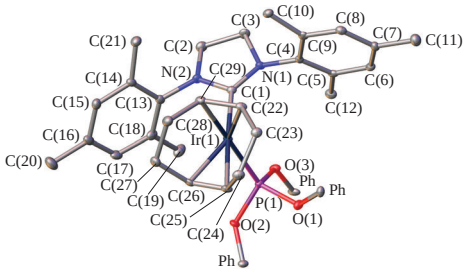

Figure 1 General view of the complex **1** in representation of atoms *via* thermal ellipsoids at 50% probability level. Hydrogen atoms and a tetrafluoroborate anion are omitted for clarity. Selected bond lengths (Å) are: Ir(1)–C(1) 2.079(3), Ir(1)–C(22) 2.167(3), Ir(1)–C(25) 2.255(3), Ir(1)–C(26) 2.178(3), Ir(1)–C(29) 2.212(3), Ir(1)–P(1) 2.2391(9), P(1)–O(1) 1.610(2), P(1)–O(2) 1.613(2), P(1)–O(3) 1.603(2).

To evaluate the efficiency of the obtained complexes **1** and **2** as iridium-based catalysts for the SABRE technique, polarization transfer from parahydrogen to these complexes and, thereby, to the coordinated pyridine ligand was studied by a repeated bubbling of parahydrogen through the methanol-d_4 solutions of **1** and **2** (in the latter case, as a pure complex $[Ir(COD)P(OPh)_3(SIPr)][BF_4]$) in the presence of pyridine, followed by acquisition of ^1H spectra [Figure 2(*a*)]. Several new signals that appeared in the range of negative chemical shifts in these spectra suggested the formation of hydride intermediates. The antiphase nature of the new signals and of the signals attributed to free and coordinated pyridine species confirmed the transfer of the spin order from the parahydrogen molecule to complexes **1** and **2**.

Although the detailed analysis of several occurring dynamics processes, including interconversion of the compounds with a different number of coordinated pyridine and methanol species, is beyond the scope of this communication, a tentative assignment of the major NMR signals can be made [Figure 2(*b*)] by comparing them with those reported in literature.[28] Note that complex **1**, despite having a significantly different N-heterecyclic carbene as a ligand, demonstrates an almost identical behaviour of the NMR spectra (see Online Supplementary Materials, Figure S2) to one observed for complex **2** upon bubbling the parahydrogen through the solution (see Figure 2).

For these new iridium complexes, we have also demonstrated the feasibility of the SABRE experiment, *i.e.*, the efficient polarization of the substrate, which subsequently dissociated from the complex giving rise to the hyperpolarization of the free substrate pool. The NMR spectra from the SABRE approach for complex **2** are shown in Figure 3. The parahydrogen was bubbled

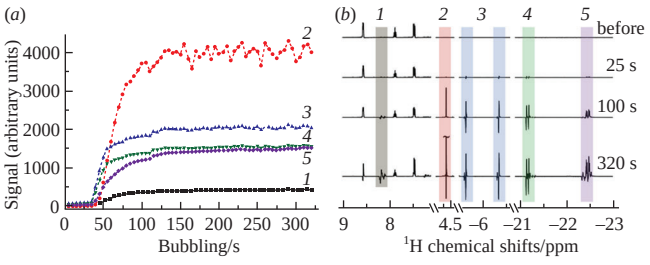

Figure 2 Polarization transfer from the parahydrogen molecule to complex **2**. (*a*) Integral intensity of the selected signals *vs.* time of parahydrogen bubbling. (*b*) 400 MHz ^1H NMR spectra obtained by a $\pi/4$ pulse before bubbling parahydrogen through a 2 mM CD_3OD solution of **2** in the presence of 40 mM pyridine and after 25, 100 and 320 seconds of bubbling. Assignments: (*1*) – *ortho*-proton of the coordinated pyridine species, (*2*) – orthohydrogen, (*3*) – hydride complex after the dissociation of the phosphite moiety, (*4*) and (*5*) – hydride complexes with a different number of coordinated methanol and pyridine species.

‡ Single crystals suitable for X-ray diffraction analysis were grown by a diffusion of Et_2O vapor into acetonitrile solutions in air.

Crystal data for **1**. $C_{47}H_{53}BF_4IrN_2O_3P$, M = 1003.89, monoclinic, space group $P2_1/n$, at 120 K: a = 9.7369(4), b = 24.0336(11) and c = 17.8723(8) Å, β = 95.1240(10)°, V = 4165.6(3) Å^3, Z = 4, d_{calc} = 1.601 g cm^{-3}, $F(000)$ = 2024. Intensities of 51626 reflections were measured [λ(MoKα) = 0.71073 Å, μ(MoKα) = 33.06 cm^{-1}, ω-scans, $2\theta < 58°$], and 11096 independent reflections (R_{int} = 0.0739) were used for the structure solution and refinement. Final R factors: R_1 = 0.0337 for 8640 observed reflections with $I > 2\sigma(I)$, wR_2 = 0.0719 and GOF = 1.011 for all the independent reflections.

Crystal data for **2**. $C_{402}H_{519}B_7F_{28}Ir_8N_{16}O_{26}P_8$, M = 8384.33, monoclinic, space group $P2_1/n$, at 120 K: a = 10.6985(10), b = 46.609(4) and c = 19.8520(18) Å, β = 92.643(2)°, V = 9888.6(16) Å^3, Z = 1, d_{calc} = 1.408 g cm^{-3}, $F(000)$ = 4274. Intensities of 87369 reflections were measured [λ(MoKα) = 0.71073 Å, μ(MoKα) = 27.88 cm^{-1}, ω-scans, $2\theta < 52°$], and 19445 independent reflections (R_{int} = 0.1010) were used for the structure solution and refinement. Final R factors: R_1 = 0.0717 for 15267 observed reflections with $I > 2\sigma(I)$, wR_2 = 0.1566 and GOF = 1.111 for all the independent reflections.

Data were obtained using a Bruker APEX2 DUO CCD diffractometer. Using Olex2,[33] the structures were solved with the ShelXT[34] structure solution program using Intrinsic Phasing and refined with the XL[35] refinement package using Least-Squares minimisation. Alkene hydrogen atoms in the coordinated COD ligands were located from difference Fourier synthesis, positions of other hydrogen atoms were calculated, and they all were refined in the isotropic approximation within the riding model. The disordered solvent molecules of acetonitrile and diethyl ether (except one that was too close to a $P(OPh)_3$ ligand in a superposition with a $P(OPh)_2(OH)$ ligand of the complex) using a Solvent Mask option as implemented in Olex2.

CCDC 2048357 and 2048358 contain the supplementary crystallographic information for **1** and **2**, respectively. These data can be obtained free of charge *via* http://www.ccdc.cam.ac.uk.

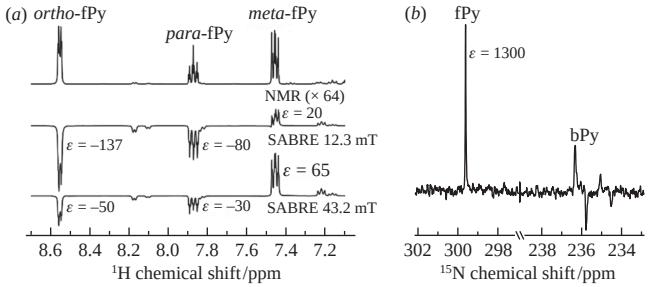

Figure 3 (*a*) ^{1}H spectra for complex **2** in CD_3OD after the SABRE polarization transfer at the field of 12.3 and 43.2 mT; a thermal NMR spectrum (multiplied by 64) shown for comparison. (*b*) ^{15}N spectrum collected using the natural isotope abundance after the SABRE polarization transfer at the field of 600 nT. Signal enhancement factors (ε) are given near the corresponding lines in the NMR spectra; fPy and bPy stand for the free and complex-bound pyridine species, respectively.

through its solution in methanol-d_4 at a low or an ultralow field, at which the transfer of the spin order to the substrate spins is efficient,[36,37] while for the NMR signal detection, a high field of 9.4 T was used. As a result, a sizeable signal enhancement was observed for complex **2**, with the respective signal enhancement factors ε being over 100 for ^{1}H nuclei and over 1000 for ^{15}N nuclei that are the same order as those, reported previously for other phosphorus-containing iridium complexes.[27]

This result highlights that introducing a phosphite ligand into a well-known SABRE catalyst is a simple way to modify the parameters of the polarization transfer from the parahydrogen molecule to both the hydride intermediates complexes and the free pyridine species. Therefore, it may provide a possibility for a full description of processes occurring in a solution upon binding the parahydrogen molecule and of the subsequent steps resulting in the polarization transfer through a detailed investigation of the NMR signals for the hydride intermediates and the use of non-coordinating solvents to minimize the number of side-processes. Parahydrogen-induced polarization thus provides an insight into dynamic transformations of metal NHC complexes, which is a topic of much interest in catalysis and related fields.[38–40] These studies are currently underway in our groups.

This work was supported by the Russian Science Foundation under collaborative interdisciplinary projects nos. 20-62-47038 and 20-63-47107. The authors also acknowledge the Russian Ministry of Science and Higher Education for providing access to NMR facilities at ITC SB RAS and to the equipment of the Center for molecule composition studies at INEOS RAS.

Online Supplementary Materials

Supplementary data associated with this article can be found in the online version at doi: 10.1016/j.mencom.2021.07.012.

References

1 J. H. Ardenkjær-Larsen, B. Fridlund, A. Gram, G. Hansson, L. Hansson, M. H. Lerche, R. Servin, M. Thaning and K. Golman, *Proc. Natl. Acad. Sci. U. S. A.*, 2003, **100**, 10158.
2 D. A. Hall, D. C. Maus, G. J. Gerfen, S. J. Inati, L. R. Becerra, F. W. Dahlquist and R. G. Griffin, *Science*, 1997, **276**, 930.
3 M. S. Albert, G. D. Cates, B. Driehuys, W. Happer, B. Saam, C. S. Springer, Jr. and A. Wishnia, *Nature*, 1994, **370**, 199.
4 I. V. Koptyug, *Mendeleev Commun.*, 2013, **23**, 299.
5 J. Kurhanewicz, D. B. Vigneron, K. Brindle, E. Y. Chekmenev, A. Comment, C. H. Cunningham, R. J. DeBerardinis, G. G. Green, M. O. Leach, S. S. Rajan, R. R. Rizi, B. D. Ross, W. S. Warren and C. R. Malloy, *Neoplasia*, 2011, **13**, 81.
6 S. E. Day, M. I. Kettunen, F. A. Gallagher, D.-E. Hu, M. Lerche, J. Wolber, K. Golman, J. H. Ardenkjaer-Larsen and K. M. Brindle, *Nat. Med.*, 2007, **13**, 1382.
7 J. Natterer and J. Bargon, *Prog. Nucl. Magn. Reson. Spectrosc.*, 1997, **31**, 293.
8 R. A. Green, R. W. Adams, S. B. Duckett, R. E. Mewis, D. C. Williamson and G. G. R. Green, *Prog. Nucl. Magn. Reson. Spectrosc.*, 2012, **67**, 1.
9 K. V. Kovtunov, E. V. Pokochueva, O. G. Salnikov, S. F. Cousin, D. Kurzbach, B. Vuichoud, S. Jannin, E. Y. Chekmenev, B. M. Goodson, D. A. Barskiy and I. V. Koptyug, *Chem. – Asian J.*, 2018, **13**, 1857.
10 J. B. Hövener, A. N. Pravdivtsev, B. Kidd, C. R. Bowers, S. Glöggler, K. V. Kovtunov, M. Plaumann, R. Katz-Brull, K. Buckenmaier, A. Jerschow, F. Reineri, T. Theis, R. V. Shchepin, S. Wagner, P. Bhattacharya, N. M. Zacharias and E. Y. Chekmenev, *Angew. Chem., Int. Ed.*, 2018, **57**, 11140.
11 C. R. Bowers and D. P. Weitekamp, *J. Am. Chem. Soc.*, 1987, **109**, 5541.
12 M. G. Pravica and D. P. Weitekamp, *Chem. Phys. Lett.*, 1988, **145**, 255.
13 L.-S. Bouchard, K. V. Kovtunov, S. R. Burt, M. S. Anwar, I. V. Koptyug, R. Z. Sagdeev and A. Pines, *Angew. Chem., Int. Ed.*, 2007, **46**, 4064.
14 R. W. Adams, J. A. Aguilar, K. D. Atkinson, M. J. Cowley, P. I. P. Elliott, S. B. Duckett, G. G. R. Green, I. G. Khazal, J. López-Serrano and D. C. Williamson, *Science*, 2009, **323**, 1708.
15 P. J. Rayner and S. Duckett, *Angew. Chem., Int. Ed.*, 2018, **57**, 6742.
16 D. A. Barskiy, S. Knecht, A. V. Yurkovskaya and K. L. Ivanov, *Prog. Nucl. Magn. Reson. Spectrosc.*, 2019, **114**–**115**, 33.
17 K. D. Atkinson, M. J. Cowley, S. B. Duckett, P. I. P. Elliott, G. G. R. Green, J. Lopez-Serrano, I. G. Khazal and A. C. Whitwood, *Inorg. Chem.*, 2009, **48**, 663.
18 M. J. Cowley, R. W. Adams, K. D. Atkinson, M. C. R. Cockett, S. B. Duckett, G. G. R. Green, J. A. B. Lohman, R. Kerssebaum, D. Kilgour and R. E. Mewis, *J. Am. Chem. Soc.*, 2011, **133**, 6134.
19 B. J. A. van Weerdenburg, N. Eshuis, M. Tessari, F. P. J. T. Rutjes and M. C. Feiters, *Dalton Trans.*, 2015, **44**, 15387.
20 P. Pham and C. Hilty, *Chem. Commun.*, 2020, **56**, 15466.
21 P. J. Rayner, P. Norcott, K. M. Appleby, W. Iali, R. O. John, S. J. Hart, A. C. Whitwood and S. B. Duckett, *Nat. Commun.*, 2018, **9**, 4251.
22 B. J. Tickner, R. O. John, S. S. Roy, S. J. Hart, A. C. Whitwood and S. B. Duckett, *Chem. Sci.*, 2019, **10**, 5235.
23 B. J. Tickner, O. Semenova, W. Iali, P. J. Rayner, A. C. Whitwood and S. B. Duckett, *Catal. Sci. Technol.*, 2020, **10**, 1343.
24 B. J. A. van Weerdenburg, A. H. J. Engwerda, N. Eshuis, A. Longo, D. Banerjee, M. Tessari, C. F. Guerra, F. P. J. T. Rutjes, F. M. Bickelhaupt and M. C. Feiters, *Chem. – Eur. J.*, 2015, **21**, 10482.
25 C. M. Wong, M. Fekete, R. Nelson-Forde, M. R. D. Gatus, P. J. Rayner, A. C. Whitwood, S. B. Duckett and B. A. Messerle, *Catal. Sci. Technol.*, 2018, **8**, 4925.
26 D. A. Barskiy, A. N. Pravdivtsev, K. L. Ivanov, K. V. Kovtunov and I. V. Koptyug, *Phys. Chem. Chem. Phys.*, 2016, **18**, 89.
27 J. F. P. Colell, A. W. J. Logan, Z. Zhou, J. R. Lindale, R. Laasner, R. V. Shchepin, E. Y. Chekmenev, V. Blum, W. S. Warren, S. J. Malcolmson and T. Theis, *Chem. Commun.*, 2020, **56**, 9336.
28 M. Fekete, O. W. Bayfield, S. B. Duckett, S. Hart, R. E. Mewis, N. Pridmore, P. J. Rayner and A. Whitwood, *Inorg. Chem.*, 2013, **52**, 13453.
29 J. A. Brown, A. R. Cochrane, S. Irvine, W. J. Kerr, B. Mondal, J. A. Parkinson, L. C. Paterson, M. Reid, T. Tuttle and S. Andersson, *Adv. Synth. Catal.*, 2014, **356**, 3551.
30 K. Ogata, T. Nagaya and S.-i. Fukuzawa, *J. Organomet. Chem.*, 2010, **695**, 1675.
31 A. R. Kennedy, W. J. Kerr, R. Moir and M. Reid, *Org. Biomol. Chem.*, 2014, **12**, 7927.
32 J. Fawcett, D. A. Harding, E. G. Hope, K. Singh and G. A. Solan, *Dalton Trans.*, 2010, **39**, 10781.
33 O. V. Dolomanov, L. J. Bourhis, R. J. Gildea, J. A. K. Howard and H. Puschmann, *J. Appl. Crystallogr.*, 2009, **42**, 339.
34 G. M. Sheldrick, *Acta Crystallogr.*, 2015, **A71**, 3.
35 G. M. Sheldrick, *Acta Crystallogr.*, 2008, **A64**, 112.
36 A. N. Pravdivtsev, A. V. Yurkovskaya, H.-M. Vieth, K. L. Ivanov and R. Kaptein, *ChemPhysChem*, 2013, **14**, 3327.
37 A. S. Kiryutin, A. V. Yurkovskaya, H. Zimmermann, H.-M. Vieth and K. L. Ivanov, *Magn. Reson. Chem.*, 2018, **56**, 651.
38 V. M. Chernyshev, E. A. Denisova, D. B. Eremin and V. P. Ananikov, *Chem. Sci.*, 2020, **11**, 6957.
39 V. A. Kirkina, E. S. Osipova, O. A. Filippov, G. A. Silantyev, D. Gelman, E. S. Shubina and N. V. Belkova, *Mendeleev Commun.*, 2020, **30**, 276.
40 E. S. Osipova, O. A. Filippov, E. S. Shubina and N. V. Belkova, *Mendeleev Commun.*, 2019, **29**, 121.

Received: 8th December 2020; Com. 20/6389